Surface & Coatings Technology 357 (2019) 879–885

Contents lists available at ScienceDirect

Surface & Coatings Technology

journal homepage: www.elsevier.com/locate/surfcoat

# Floating harmonic probe for diagnostic of pulsed discharges

M. Zanáška[a,b,*], Z. Turek[a], Z. Hubička[b], M. Čada[b], P. Kudrna[a], M. Tichý[a]

[a] Charles University, Faculty of Mathematics and Physics, Prague, Czech Republic
[b] Institute of Physics, Academy of Sciences of the Czech Republic, Prague, Czech Republic

ARTICLE INFO

*Keywords:*
Floating harmonic probe
Phase delay harmonic analysis method
Double floating harmonic probe
Pulsed discharge

ABSTRACT

The floating harmonic probe (FHP) is a relatively new plasma diagnostic method for electron temperature and positive ion density measurement, which can be used in conditions when insulating films are being deposited on the probe and, consequently, the classical Langmuir probe method fails. Recently an extension of this method called PDHAM – phase delay harmonic analysis method - was proposed that is applicable also to pulsed discharges. In this contribution, we study the possible limitations of this new method and present the comparison of the plasma density and the electron temperature determined by PDHAM with that obtained by the time-resolved Langmuir probe in a pulsed planar magnetron discharge. In addition, we present the double probe technique for applications in pulsed plasmas and we compare its results with those of a single FHP. The experiments were performed in argon at pressures several Pa in a non-reactive regime, when no insulating film was deposited on the probes.

## 1. Introduction

The low-pressure discharge plasma is widely used in many advanced technological processes such as in anisotropic etching or thin film deposition, see e.g. the overview in [1]. The knowledge of plasma parameters, preferably measured in-situ during the actual technological process, is a key for its understanding and, also, for its control in real-time. The electron temperature, electron density or ion density and ion flux are among the critical internal parameters that should be monitored. Consequently, there is still a need for development of the reliable measurement techniques.

The most widely used electric probes in low-temperature plasmas are the Langmuir probes (LP). Many important plasma parameters can be extracted from the IV characteristics of the single Langmuir probe, such as the electron and ion density, electron temperature or the electron energy distribution function (EEDF). However, its applicability during reactive sputtering of non-conducting films is highly constricted, as the IV characteristic get distorted and, consequently, its processing is complicated, unreliable and often impossible. A range of probe methods that operate with an ac voltage has been developed to overcome this problem. One group of these methods is based on the high-frequency/microwave spectroscopy. In case of the passive plasma resonance spectroscopy the probe works as antenna that monitors existing oscillations of the plasma, in the active plasma resonance spectroscopy the probe couples a suitable RF signal into the plasma and evaluates the corresponding frequency response [2,3]. As a representative of the first group may serve e.g. the plasma oscillation probe [4], examples of the second group are the plasma impedance probe [5], the hairpin probe [6], the multipole resonance probe [7] and the curling probe [8]. All the mentioned probe methods determine the electron density. The multipole resonance probe [7] can measure also the electron temperature and the plasma collision frequency, however, it ceases working when only a few nm conducting film is deposited on the probe [9]. Advantage of these methods is a possibility to monitor the plasma technological process (deposition, sterilization etc.) in-situ continuously, without the need to measure and process the probe characteristic. Disadvantage of these methods is the need of microwave instrumentation (a vector network analyzer), large size and a comparatively complicated construction of all the probes listed above. As a probe that utilizes an ac voltage at the RF frequency we mention the probe method for ion flux measurements [10]. This method is almost independent on the thickness of the non-conducting layer on the probe; however, for the method to work properly it is necessary to have a large flat probe (in [10] the diameter of the probe was 50 mm).

The idea to couple an ac signal into the dc probe bias has been discovered long time ago. As an example of application of this idea may serve the works [11,12] where a second harmonic of a harmonic signal coupled into the probe circuit was used to measure the electron energy distribution function in a plasma of a striated discharge. The concept of the so-called floating harmonic probe (FHP), i.e. of a method where

* Corresponding author at: Charles University, Faculty of Mathematics and Physics, Prague, Czech Republic.
*E-mail address:* zanaska@fzu.cz (M. Zanáška).

https://doi.org/10.1016/j.surfcoat.2018.10.039
Received 29 June 2018; Received in revised form 11 October 2018; Accepted 15 October 2018
Available online 18 October 2018
0257-8972/ © 2018 Elsevier B.V. All rights reserved.

only an ac signal is applied to the probe over a capacitor, was proposed already in [13] and was originally intended for direct-display of the electron temperature fluctuations in the edge plasma of tokamaks [14]. In [15] this technique has been extended to evaluate also the ion number density and it was proposed to be used in low-temperature processing plasmas, where the probe tip gets coated by an insulating layer. Up to now the FHP has been found useful e.g. during deposition of DLC thin films [16,17] and was tested and utilized during reactive sputtering of hematite dielectric films in dc hollow cathode plasma jet sputtering system [18]. The case when the capacitive reactance of the deposited film is not negligible was treated in [19,20]. Further variation on the FHP is a method using sideband harmonics generated by dual-frequency input voltage [21,22].

In this work, we are building mainly on the concept of the single FHP applied to pulsed plasmas proposed in [23]. Our work was motivated by the increasing interest in scientific community in HiPIMS, see e.g. the recent reviews [24,25]. Moreover, we present the double floating harmonic probe technique [26] for applications in pulsed plasmas and compare the plasma parameters obtained by this method with those of the single FHP.

## 2. Theory

### 2.1. Theory of single FHP operation in pulsed plasmas

The principle and theory of FHP for pulsed plasmas is similar to that used in continuously driven discharges, see [15]. A small ac voltage $V_0 \cos \omega t$ of a given frequency is applied to the probe electrode with respect to a vacuum vessel in contact with plasma. As long as the capacitance of the deposited insulating film on the probe is high enough, it doesn't affect the ac probe current being measured. A dc blocking capacitor $C_b$ is connected between the probe and the harmonic voltage source so that no dc current can flow through the probe. In continuously driven dc discharges, where the plasma is stationary and the plasma potential is independent on time, the probe current is solely generated by the applied ac voltage sweeping around the probes mean potential $\overline{V}$ which is very close to the local floating potential. However, in pulsed discharges the plasma potential variations (and accordingly variations of the local floating potential) during the pulse period can cause the probe not to be able to follow the local floating potential changes and the probe transient voltage $V_t$ and transient current $i_t$ must be taken into account. Let's first assume that the frequency of the ac voltage is high enough, so that the plasma parameters do not significantly change during several ac voltage periods. The probe current is assumed to be a sum of the positive ion current and the electron current:

$$i = -i^+ + i^- \exp[(\overline{V} + V_t + V_0 \cos \boldsymbol{\omega} t - \boldsymbol{\Phi}_{pl})/T_e] \quad (1)$$

where $i^-$ is the electron current when the probe voltage equals the plasma potential $\Phi_{pl}$ and $e$ is the elementary charge. The ion current $i^+$ is supposed to be independent on the probe voltage and the EEDF is assumed to be Maxwellian with temperature $T_e$. To make the equations easier to follow, we expressed in Eq. (1) as well as further in the text the electron temperature in electron-volts. After expansion of the exponential in a Fourier series, the probe current reads [23]:

$$i = -i_t + \sum_{k=1}^{\infty} i_{k\boldsymbol{\omega}} \cos k\boldsymbol{\omega} t, \quad (2)$$

$$i_t = -i^+ + i^- \exp\left(\frac{\overline{V} + V_t - \boldsymbol{\Phi}_{pl}}{Te}\right) I_0\left(\frac{V_0}{T_e}\right), \quad (3)$$

$$i_{k\boldsymbol{\omega}} = 2i^- \exp\left(\frac{\overline{V} + V_t - \boldsymbol{\Phi}_{pl}}{Te}\right) I_k\left(\frac{V_0}{T_e}\right). \quad (4)$$

In these expressions $I_k$ represents the modified Bessel function of the first kind. We see that besides the current component of the fundamental frequency $\omega$, also current components of higher harmonic frequencies arise due to the non-linear characteristics of the sheath. From the analysis similar to that given in [18] follows that the electron temperature $T_e$ can be evaluated exactly in the same manner as in the continuously driven discharges from the ratio of the amplitudes of the harmonic current components $i_{k\omega}$:

$$i_{n\boldsymbol{\omega}}/i_{m\boldsymbol{\omega}} = I_n(V_0/T_e)/I_m(V_0/T_e),\ n,\ m \in \mathbb{N},\ n \neq m \quad (5)$$

From the Eqs. (2), (3) and (4) the following formula for the positive ion current $i^+$ can be derived:

$$i^+ = -i_t + i_{1\boldsymbol{\omega}} \frac{I_0(V_0/T_e)}{2I_1(V_0/T_e)}, \quad (6)$$

which differs from that used in continuously driven discharges by considering the transient current $i_t$. To obtain the ion number density the collisionless Laframboise theory [27] of the ion current for cylindrical probe was applied. According to this theory the ion current $i^+$ was expressed by an analytical formula that can be found in [28] evaluated at the probe potential $\Phi_{pl} - 5.2T_e$ (for argon plasma).

For the operation of the probe as described above, it is crucial, that the capacitance of the sheath $C_s$ can be neglected. This condition, however, limits the maximum operating frequency $\omega$ that can be used. Furthermore, the potential drop on the capacitance of the insulating film $C_f$ is in the above treatment also neglected which limits the maximum thickness of the deposited insulating film. After introducing the real part of the impedance of the sheath $R_s$ as the first derivative of the probe IV characteristics at the probe potential $\overline{V} + V_t - \boldsymbol{\Phi}_{pl}$ around which the FHP in a pulsed plasma operates, $R_s^{-1} = \frac{dI}{dV}(\overline{V} + V_t - \boldsymbol{\Phi}_{pl})$ [29], the range of operating frequencies of the floating harmonic probe can be expressed by:

$$\boldsymbol{\omega} C_f C_b/(C_f + C_b) \gg \frac{1}{R_s} \gg \boldsymbol{\omega} C_s \quad (7)$$

That is formally the same expression as derived in [18]; moreover, it takes into account also the impedance of the blocking capacitor.

### 2.2. Theory of double FHP operation

The principle of the double FHP method [26] is similar to the single FHP and is based on the theory of double probe developed already by Johnson and Malter [30]. An ac harmonic voltage $V_0 \cos \omega t$ is applied between two probes of equal size positioned near each other in plasma. Assuming an ideal double probe characteristics (Maxwellian EEDF, constant ion current $i^+$) the probe current is given by

$$i = i^+ \tanh \frac{\boldsymbol{\Delta} V_f + V_0 \cos \boldsymbol{\omega} t}{2T_e}, \quad (8)$$

where $\Delta V_f$ denotes the difference of the floating potentials of the two probes caused mainly by the spatial difference of plasma potential. This potential difference depends on the distance between the two probes; the closer the probes the lower $\Delta V_f$. In general, however, if a capacitor is connected in series with the ac voltage source, it will get charged by plasma to compensate this difference and then the formula (8) with $\Delta V_f = 0$ can be used.

Assuming that the ac voltage amplitude is small compared to the electron temperature ($V_0 \ll T_e$) then the procedure described in [26] can be applied and the probe current (8) can be expanded into Taylor series and separated into harmonic components:

$$i/i^+ = \left(a - \frac{a^3}{4} + \ldots\right) \cos \boldsymbol{\omega} t + \left(-\frac{a^3}{12} + \ldots\right) \cos 3\boldsymbol{\omega} t + \ldots \quad (9)$$

where $a = V_0/2T_e$ and the terms with power higher than $a^4$ were neglected.

It then follows that the electron temperature can be evaluated from the ratio R of the amplitudes of the third and the first harmonic current components, $R = i_{3\omega}/i_{1\omega}$:

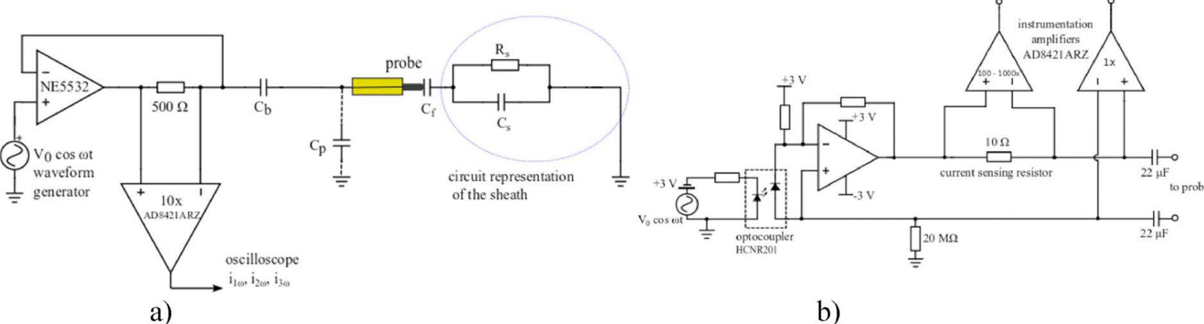


**Fig. 1.** a) The schema of the single FHP measuring circuit including the linearized circuit representation of the sheath around the probe, the parasitic capacitance $C_p$ and the capacitance $C_f$ of an insulating film. b) The schema of the double FHP measuring circuit.

$$\frac{T_e}{V_0} = \sqrt{\frac{3R+1}{48R}} \tag{10}$$

and the ion current from the amplitude of the first harmonic current component $i_{1\omega}$:

$$i^+ = \frac{i_{1\omega}}{a - \frac{a^3}{4}} \tag{11}$$

The ion number density is obtained in the same way as in the single FHP case. In appendix A we analyze also the case when $V_0 > T_e$ and study the range of validity of the $V_0 \ll T_e$ treatment.

In the double FHP theory shown above it is assumed that the currents through both the probes are equal and of opposite sign at any time, so that the measured current flows almost exclusively through both the probes and the transient/charging currents are negligible. In order to apply the double probe in the pulsed regime it is therefore necessary for the double probe to follow closely the local floating potential changes. That is only possible, if the “RC constant” given by the product of the sheath impedance and the sum of the capacitances of the probes and of the measuring circuit to ground is negligibly small.

### *2.3. Phase delay harmonic analysis method*

Due to the sheath capacitance (and partially also due to the parasitic capacitances of the measuring circuitry and electrical leads to the probe) the operating frequency of the input ac voltage is limited to about 100 kHz [18]. Even if just one period of the applied signal was used to evaluate the plasma parameters, the temporal resolution in this case couldn't be better than about 10 μs, which is still too much to reliably capture the changes during 100 μs HiPIMS (High-Power Impulse Magnetron Sputtering) pulse.

An alternative measurement technique named PDHAM – Phase Delay Harmonic Analysis Method was recently proposed in [23]. Similarly to the conventional time-resolved Langmuir probe method (sometimes called the box-car LP method), it is assumed that the plasma is generated repeatedly with reproducible parameters and that, consequently, measurement during several discharge periods can be used for obtaining the temporal evolution of the plasma parameters. In this method the ac input voltage is synchronized with the triggering signals of the discharge pulses. In the first trigger the ac voltage with no phase delay is applied to the probe and the probe current is measured. In the subsequent triggers the applied voltage is incrementally delayed by some integer phase fraction of $2\pi$. After several discharge pulses when reaching the phase delay of $2\pi$, one period of the applied voltage can be reconstructed in the phase domain at any time sampled during the discharge period. Similarly, the corresponding one period current waveform can be reconstructed in the phase domain, which is then used for the evaluation of the electron temperature and ion number density according to the theory of the FHP. The time resolution in this case is limited just by the sampling frequency during recording of the current waveforms, i.e. by the speed of the A/D converter, and by the ion plasma frequency (similarly to the conventional Langmuir probe method) and not by the applied frequency. Last but not least one has to take into account the “physical” time resolution of the Langmuir probe that is given by the time of flight of an ion through the probe sheath (numerically the reciprocal of the ion plasma frequency).

## 3. Experimental arrangement

Measurements were carried out in the pulsed dc discharge of planar magnetron with 2-inch titanium target. Argon was used as the working gas. The magnetron was powered by a pulsing unit that consists of a dc power supply Advanced Energy MDX 500 that charges the capacitor bank and of an ultrafast switch constructed from the IGBT transistors. Its basic architecture is described in [31], the detailed construction in [32]. The pulsing unit was controlled by pulses from the function generator Agilent 33521A. The rise time of the voltage applied on the cathode was lower than 200 ns. These pulses also triggered the ac voltage applied to the FHP probe.

The double probe was made of two tungsten wires of 13 mm in length and of diameter of 50 μm and was positioned at the axis of the magnetron in the distance of about 8 cm from the magnetron target. When using the single probe method, only one of the two wires was used. In the presented experiments with argon as a working gas only a conducting titanium layer was deposited on the probe which did not substantially alter the probe dimensions. Hence, the comparison of the FHP with the conventional time-resolved Langmuir probe technique was possible. The IV characteristics of the Langmuir probe were measured by means of an in-house constructed electronic circuitry, similar to that used in [33].

The electrical circuit employed for the single FHP technique is depicted in Fig. 1a. The probe current was sensed on a 500 Ω resistor and the current signal was amplified by a low noise, low bias current, high speed and high CMRR (common mode rejection ratio) differential amplifier AD8421ARZ by a factor of 10. The high CMRR allows to extract low level signals even in the presence of high-frequency common-mode noise. The negative feedback line in the operational amplifier NE5532 was hooked up at the end of the sensing resistor as depicted in Fig. 1. That ensured that only the voltage of the fundamental frequency ω was applied to the probe and the amplitudes of higher frequencies possibly generated on the sensing resistor were suppressed. To let the probe floating and self-biased a capacitor of either $C_b$ = 5 nF or 50 nF was connected in series between the measuring circuit and probe, the effect of which on the resulting data is also the subject of this study.

For the measurement with the double probe we used the electric circuitry depicted in Fig. 1b. The sinusoidal signal is applied through an optocoupler and an operational amplifier powered by two 3 V batteries. The content of higher harmonic amplitudes in the applied voltage was

lower by > 60 dB compared to the amplitude of the fundamental frequency. The current was sensed on a 10 Ω resistor, whose resistance could be neglected compared to the impedance of the sheath, and amplified by the operational amplifier powered by a grounded power supply. The net capacitance of the probes, the electrical leads (about 70 cm long) and the measuring circuit to ground was roughly 100–150 pF.

Both the single and the double FHP were operated using the phase delayed method. As a signal-recording device the digital oscilloscope Agilent DSO-X 2004A was used. In order to simultaneously study the probes operation, the floating potential was also recorded using an oscilloscopic probe with a capacity of 15 pF against ground. The harmonic signal of a given frequency was supplied by the waveform generator Agilent 33220A operated in the burst mode. The start of the burst was synchronized with the discharge triggering pulses with a programmable delay. In the burst mode only several periods of the harmonic input voltage were generated after the pulse trigger covering most of the discharge repetition period. After several discharge periods the phase/delay of the signal burst was readjusted in pre-programmed steps. The data acquisition terminated when the phase/delay reached 360°. From the current waveforms in the time domain the waveforms in the phase domain were then constructed, from which the amplitudes of the harmonic currents were obtained by means of the Fourier analysis. Both the waveform generator and the oscilloscope were connected to a computer, which automatically controlled the incremental change of the input voltage phase and retrieved the waveform data from oscilloscope.

## 4. Results and discussion

The results presented below have been measured at the following conditions: a frequency of 20 kHz and ac voltage amplitude of 0.4 V was used for FHP measurement, discharge conditions: pressure = 1 Pa, average discharge current = 250 mA, discharge voltage = 400 V, average discharge power = 100 W, pulsing frequency = 100 Hz, duty cycle = 10%.

In Fig. 2a, b two examples of the results of comparative measurements of the ion/electron number density and the electron temperature by both the FHP (using the phase delay technique) and the time-resolved Langmuir probe during and after a 1 millisecond long discharge pulse are shown, respectively. Furthermore, FHP results obtained during measurement with two different dc blocking capacitors $C_b$ are also compared. To understand why the results may depend on the capacitance of the dc blocking capacitor used, the temporal evolution of the potential on the FHP, local floating potential, local plasma potential and the FHP transient current is depicted in Fig. 2c, d for two different $C_b$ values. The local floating potential was measured directly by the oscilloscope probe when the probe was disconnected from the FHP circuit. We have observed a delay of about 120 μs between the time of application of the discharge voltage and the time of the plasma ignition, which is depicted in Fig. 2a, b, c, d by a gray rectangle. We observe in Fig. 2c that after that delay the local floating potential steeply increases to approximately 3.5 V, during the active pulse slightly decreases and as soon as the pulse terminates the local floating potential rapidly decreases. Similar temporal evolution was obtained also for the local plasma potential. Further is in Fig. 2c depicted the probe potential when the probe was connected to the FHP measurement circuit with the applied harmonic voltage of given phase (thin bright line) and the mean probe potential obtained by averaging the probe potential in the phase domain (thick line). Clearly, the FHP was not able to follow the rapid changes of the local floating potential as the impedance of the sheath and the dc blocking capacitor forms effectively a non-linear low-pass filter – the blocking capacitor needs to be charged by the plasma through the sheath impedance. This charging current, the transient current $i_t$, obtained by averaging the probe current in the phase domain is depicted in Fig. 2d and it is both qualitatively and quantitatively in agreement with the results. The situation becomes worse when the local floating potential increases because in such a case the probe is left in the ion saturation region where only small ion current flows onto the probe, hence the impedance of the sheath is large. On the other hand, when the local floating potential decreases the probe remains in the transition region with rather high electron current and hence the probe faster follows the changes of the local floating potential.

The electron temperature obtained with the 50 nF capacitor is burdened with scatter and its mean value is overestimated for the duration of the active time of the pulse when compared to that obtained from the LP data, as shown in Fig. 2b. It has to be noted that during the first 120 μs after start of the voltage, the FHP temperature data for both the capacitors shown are not valid; they represent just noise. When the 5 nF capacitor was used, the temperature was overestimated only at the beginning of the voltage pulse to about 400 μs. The reason lies in the FHP mean potential that differs from the local floating potential. We see that the electron temperature is overestimated only when the FHP mean potential is much lower than the local floating potential. Consequently, the FHP was operating far in the ion saturation region, where the electron current and the corresponding harmonic currents are much smaller and hence almost lost in noise. Furthermore, the tail of the EEDF may not be Maxwellian anymore and the dependence of the ion current on voltage may also play a role, as the ion current - in this part of the IV characteristic - is much higher than the electron current. The rather low value of electron temperature during the active plasma pulse was observed also in other papers dealing with Langmuir probe diagnostics of pulsed plasma discharge [34–36].

When assessing the ion density from FHP measured with both capacitors in Fig. 2a, it is overestimated with respect to the electron density obtained from Langmuir probe. The difference might be due to the imperfection of the Laframboise theory commonly observed also in other experiments, e.g. [37]. We see that although the probe with 50 nF dc blocking capacitor used was absolutely not able to follow the changes of the local floating potential during the active pulse, the ion density obtained with 50 nF capacitor is roughly similar to the results when the 5 nF capacitor was used. However, we consider the measurement of the temporal evolution of the ion density during the active pulse with the 50 nF dc blocking capacitor as unreliable. That is mainly due to the fact, that the electron temperature, which is needed for the ion density evaluation, was too noisy.

From the results we conclude that the lower capacitance of the dc blocking capacitor enables the faster response of the probe to the changes of the local floating potential and hence leads to more reliable data. However, the condition for proper operation of the FHP expressed in Eq. (7) limits the minimum capacitance of the dc blocking capacitor. The optimal value of the dc capacitor should therefore take into account the size of the probe and the maximum densities expected during the pulse. The fact that the sheath impedance actually depends on the probe transient voltage further complicates the choice.

In view of the above mentioned inherent problem of the single FHP when used in pulsed discharges, we have focused on the applicability of the double FHP, because no dc blocking capacitor connected to ground is needed in this technique. The measurements comparing the single and double FHP have been made measured at the following conditions: a frequency of 20 kHz and ac voltage amplitude of 0.4 V and 0.45 V was used for the single FHP and double FHP, respectively, discharge conditions: pressure = 10 Pa, average discharge current = 300 mA, discharge voltage = 285 V, pulsing frequency = 100 Hz, duty cycle = 10%.

In our measurements with double FHP we have observed only negligible transient currents and the mean potential followed perfectly the changes of the local floating potential. In Fig. 3b one can observe that the electron temperature obtained with double FHP is in rather good agreement with that obtained from LP even in the first 500 μs from the beginning of the pulse, while the electron temperature from the single FHP is overestimated. The ion density determined by both the

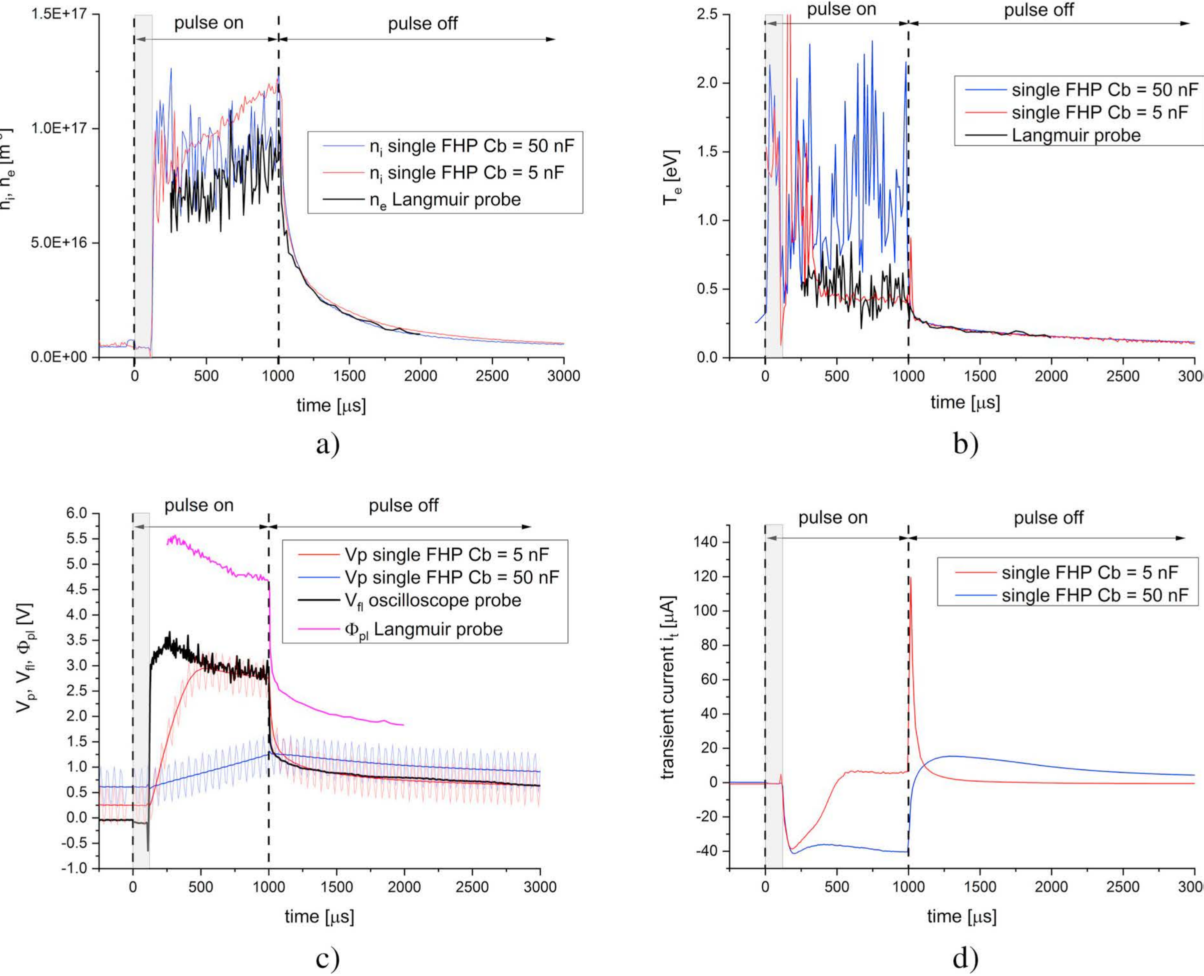


**Fig. 2.** Time evolution of several plasma and probe parameters during and after discharge pulse. Two different dc blocking capacitors of 5 nF and 50 nF were used for FHP (PDHAM) measurement. (a) Ion density measured by FHP and electron density measured by Langmuir probe obtained from the probe current at the plasma potential (b) Electron temperature from FHP determined from the ratio $i_{1\omega}/i_{2\omega}$, electron temperature by Langmuir probe determined from the slope of 2nd derivative of the IV characteristic. (c) $V_p$ - the FHP potential during measurement and its mean value. $V_{fl}$ - the floating potential of the probe not connected to FHP measuring circuit, $\Phi_{pl}$ – plasma potential measured by Langmuir probe. (d) The transient current $i_t$ flowing through the FHP probe. A frequency of 20 kHz and ac voltage amplitude of 0.4 V was used for FHP measurement. Discharge conditions: pressure = 1 Pa, average discharge current = 250 mA, discharge voltage = 400 V, average discharge power = 100 W, pulsing frequency = 100 Hz, duty cycle = 10%.

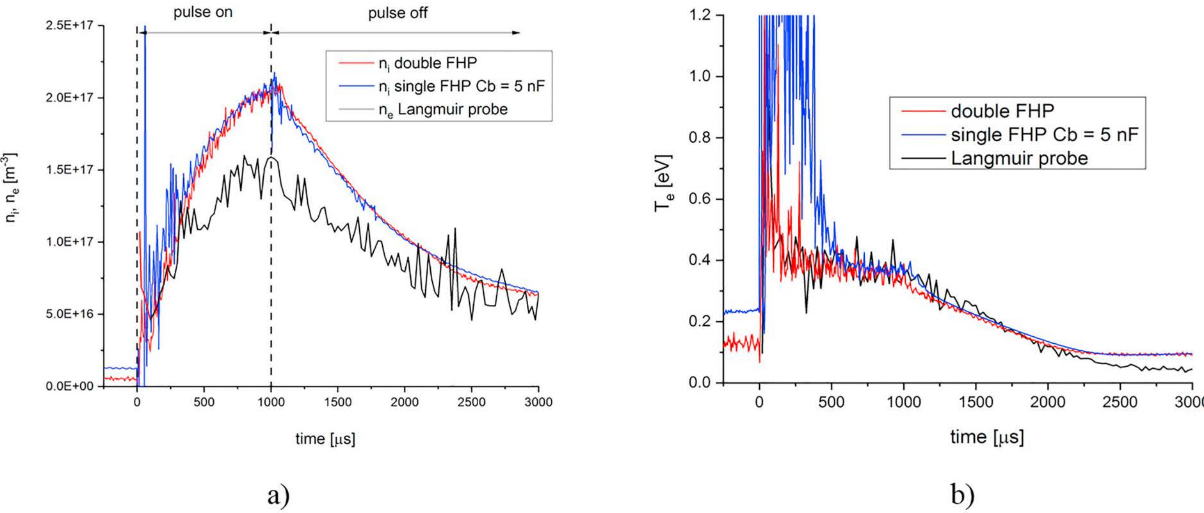


**Fig. 3.** Comparison of the ion and electron density (a) and electron temperature (b) as measured by the single FHP, double FHP and time-resolved Langmuir probe. A frequency of 20 kHz and ac voltage amplitude of 0.4 V and 0.45 V was used for single FHP and double FHP measurement, respectively. Discharge conditions: pressure = 10 Pa, average discharge current = 300 mA, discharge voltage = 285 V, pulsing frequency = 100 Hz, duty cycle = 10%.

single and double FHP techniques are in good agreement; it, however, differs from the electron density for the same reason as explained above.

## 5. Conclusion

We have tested and studied a relatively new probe diagnostic technique called the PDHAM, which is intended for electron temperature and positive ion number density measurement in pulsed discharges during reactive sputtering even when the probe is covered by an insulating film. The probe was tested in dc pulsed planar magnetron discharge commonly used for reactive deposition of dielectric films. The temporal evolution of electron temperature and ion density was measured using this technique and compared with time-resolved Langmuir probe results at several different discharge conditions in non-reactive regime. We have obtained good agreement of the PDHAM with conventional Langmuir probe method. Furthermore, the measurement with the PDHAM was several times faster and the results were less noisy when compared to the time-resolved Langmuir probe technique. It was showed that the results and the probe reliability can highly depend on the dc blocking capacitor used and on the particular temporal evolution of the local floating potential. Due to this fact, it is not generally guaranteed that the PDHAM/FHP will provide reliable data even if the optimal dc blocking capacitor was used. We demonstrated that the reliability of the plasma parameters data could depend, apart from the capacity of the dc blocking capacitor also on the particular temporal evolution of the local floating potential. Due to this fact, the PDHAM/FHP might not provide reliable data even if one chooses the optimal value of the dc blocking capacitor.

We have shown that the solution of this problem might provide the double floating harmonic probe technique. This technique does not require a dc blocking capacitor, the sheath impedance is well defined and, consequently, the method yields reliable data of the electron temperature and the ion density.

In the future, we plan to apply the PDHAM/FHP in the HiPIMS discharge; also during deposition. The preliminary results show better reliability of the double floating harmonic probe technique also in these experimental conditions.

## Acknowledgments

The partial financial support by EUROfusion and by the Charles University Grant Agency, grant no. 1188218 is greatly acknowledged. The work was supported by Operational Programme Research, Development and Education financed by European Structural and Investment Funds and the Czech Ministry of Education, Youth and Sports (Project No. SOLID21 - CZ.02.1.01/0.0/0.0/16_019/0000760).

## Appendix A

In this appendix we discuss the range of validity of the assumption $V_0 \ll T_e$ in the derivation of Eqs. (10) and (11) for the double FHP and show an extension applicable even for $V_0 > T_e$. We have evaluated the normalized harmonic currents $i_{1\omega}/i^+$ and $i_{3\omega}/i^+$ by expanding Eq. (8) directly into Fourier series by numerical integration of the expression for Fourier series coefficients (we remind the reader that $a = V_0/2T_e$)

$$i_{n\omega}/i^+ = 2\left|\int_0^1 \tanh(a\cos 2\pi t)\cos 2\pi nt\,dt\right| \tag{A.1}$$

Fig. A.1 shows the calculated values together with the approximations according to Eq. (9). The approximate formula (9) is in good agreement with the numerical results for $a < \approx 0.5$. At $a = 0.5$ the relative error of $i_{3\omega}/i_{1\omega}$ and $i_{1\omega}/i^+$ amounts to 13% and 0.5% respectively. We have fitted the numerical data by analytical expressions (A.2) and (A.3), which are applicable in the range $0.4 < a < 8$ with maximum relative error of 4%. One should be also aware of the fact, that a too high voltage amplitude scans the double probe characteristic over the range of voltages within which the assumptions of the simple double FHP theory are not satisfied (the ion current $i^+$ is not constant).

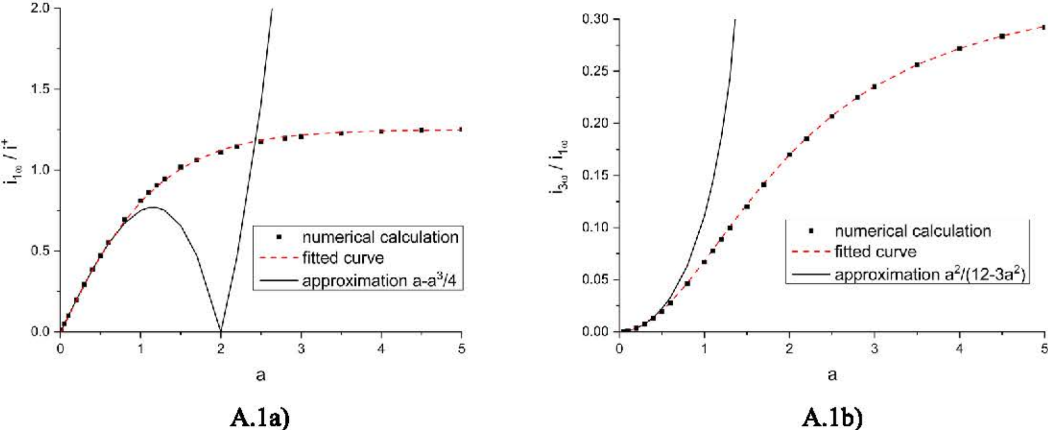


**Fig. A.1.** Comparison of the theoretical approximate harmonic current amplitudes according to Eq. (9) and those obtained from numerical integration of Eq. (A.1). The fitted approximations of the numerical data given by a) Eq. (A.3) and b) Eq. (A.2) are shown by the dashed lines.

When the measured ratio $i_{3\omega}/i_{1\omega}$ was lower than about 0.01 (corresponding to $a \approx 0.4$) the expressions (10) and (11) were used, otherwise we utilized Eq. (A.4) and (A.3) for the electron temperature and ion current evaluation, respectively.

$$R = i_{3\omega}/i_{1\omega} = 0.34\left(1 - \frac{4}{4 + a^2}\right) \tag{A.2}$$

$$i_{1\omega}/i^+ = 1.25 - 3.3/\left(1 + \exp\frac{a + 0.35}{0.73}\right) \tag{A.3}$$

$$T_e = \frac{V_0}{4}\sqrt{\frac{0.34}{R} - 1} \tag{A.4}$$

## References


[1] I. Adamovich, et al., J. Phys. D. Appl. Phys. 50 (2017) 323001.
[2] N.S.J. Braithwaite, R.N. Franklin, Plasma Sources Sci. Technol. 18 (2009) 014008.
[3] M. Lapke, J. Oberrath, Ch. Schulz, R. Storch, T. Styrnoll, Ch. Zietz, P. Awakowicz, R.P. Brinkmann, T. Musch, T. Mussenbrock, I. Rolfes, Plasma Sources Sci. Technol. 20 (2011) 042001.
[4] A. Schwabedissen, C. Soll, A. Brockhaus, J. Engemann, Plasma Sources Sci. Technol. 8 (1999) 440.f.
[5] David D. Blackwell, David N. Walker, William E. Amatucci, Rev. Sci. Instrum. 76 (2005) 023503.
[6] R.B. Piejak, V.A. Godyak, R. Garner, B.M. Alexandrovich, J. Appl. Phys. 95 (2004) 3785.
[7] Christian Schulz, Tim Styrnoll, Peter Awakowicz, Ilona Rolfes, IEEE Trans. Instrum. Meas. 64 (2015) 857.
[8] Anil Pandey, Wataru Sakakibara, Hiroyuki Matsuoka, Keiji Nakamura, Hideo Sugai, Appl. Phys. Lett. 104 (2014) 024111.
[9] T. Styrnoll, S. Bienholz, M. Lapke, P. Awakowicz, Plasma Sources Sci. Technol. 23 (2014) 025013.
[10] N.St.J. Braithwaite, J.P. Booth, G. Cunge, Plasma Sources Sci. Technol. 5 (1996) 677.
[11] R.L.F. Boyd, N.D. Twiddy, Proc. R. Soc. Lond. A 250 (1959) 53.
[12] S.W. Rayment, N.D. Twiddy, J. Phys. D. Appl. Phys. 2 (1969) 1747.
[13] R. Van Nieuwenhove, G. Van Oost, Rev. Sci. Instrum. 59 (1988) 1053.
[14] J.A. Boedo, D. Gray, R.W. Conn, P. Luong, M. Schaffer, R.S. Ivanov, A.V. Chernilevsky, G. Van Oost, The TEXTOR Team, Rev. Sci. Instrum. 70 (1999) 2997.
[15] Min-Hyong Lee, Sung-Ho Jang, Chin-Wook Chung, J. Appl. Phys. 101 (2007) 033305.
[16] Jianhua Pang, Wenqi Lu, Xin Yu, Hanghang Wang, Jia He, Jun Xu, Plasma Sci. Technol. 14 (2012) 172.
[17] Bai Yujing, Li Jianquan, Jun Xu, Wenqi Lu, Younian Wang, Ding Wanyu, Plasma Sci. Technol. 18 (2016) 58.
[18] M. Zanáška, Z. Hubička, M. Čada, P. Kudrna, M. Tichý, J. Phys. D. Appl. Phys. 51 (2) (2018) 025205.
[19] Jin-Young Bang, Kyoung Yoo, Dong-Hwan Kim, Chin-Wook Chung, Plasma Sources Sci. Technol. 20 (2011) 065005.
[20] Kyung-Hyun Kim, Dong-Hwan Kim, Chin-Wook Chung, Plasma Sources Sci. Technol. 26 (2017) 025001.
[21] S. Jang, G. Kim, C. Chung, Thin Solid Films 519 (2011) 7042.
[22] D. Kim, H. Lee, Y. Kim, C. Chung, Appl. Phys. Lett. 103 (2013) 084103.
[23] Yu-Sin Kim, Dong-Hwan Kim, Hyo-Chang Lee, Chin-Wook Chung, J. Appl. Phys. 117 (2015) 243302.
[24] A. Anders, J. Appl. Phys. 121 (2017) 171101.
[25] Y. Yuan, L. Yang, Z. Liu, Q. Chen, Plasma Sci. Technol. 20 (2018) 065501.
[26] Oh. Se-Jin, Ik-Jin Choi, Jin-Yong Kim, Chin-Wook Chung, Meas. Sci. Technol. 23 (2012) 085001.
[27] G. Laframboise, University of Toronto, Institute of Aerospace Studies (UTIAS), Report No. 100, (1966).
[28] O. Chudacek, P. Kudrna, J. Glosík, M. Šícha, M. Tichý, Contrib. Plasma Phys. 35 (1995) 503.
[29] N. Hershkowitz, How langmuir probes work, in: O. Auciello, D.L. Flamm (Eds.), Plasma Diagnostics, Vol. 1, Discharge Parameters and Chemistry, Academic Press, 1989.
[30] E.O. Johnson, L. Malter, Phys. Rev. 80 (1950) 58.
[31] K. Sarakinos, J. Alami, S. Konstantinidis, Surf. Coat. Technol. 204 (2010) 1661.
[32] V. Kučera, Bachelor Thesis, South-Bohemian University, full text on, 2015. https://theses.cz/id/c99aup/KUCERA_BP_2015.pdf.
[33] P. Kudrna, J. Kluson, S. Leshkov, et al., Contrib. Plasma Phys. 50 (9) (2010) 886–891.
[34] M. Čada, Z. Hubička, P. Adámek, J. Klusoň, L. Jastrabík, Surf. Coat. Technol. 205 (2011) S317–S321.
[35] J.T. Gudmundsson, J. Alami, U. Helmersson, Appl. Phys. Lett. 78 (2001) 3427.
[36] J.T. Gudmundsson, P. Sigurjonsson, P. Larsson, D. Lundin, U. Helmersson, J. Appl. Phys. 105 (2009) 123302.
[37] F.F. Chen, J.D. Evans, W. Zawalski, Plasma Sources Sci. Technol. 21 (2012) 055002.

IOP Publishing

Journal of Physics D: Applied Physics

J. Phys. D: Appl. Phys. 51 (2018) 025205 (8pp)

https://doi.org/10.1088/1361-6463/aa9d3b

# Floating harmonic probe measurements in the low-temperature plasma jet deposition system

M Zanáška[1], Z Hubička[2], M Čada[2], P Kudrna[1] and M Tichý[1,3,4]

[1] Charles University, Faculty of Mathematics and Physics, Ke Karlovu 3, 121 16 Prague 2, Czechia
[2] Academy of Sciences of the Czech Republic, Institute of Physics, Na Slovance 2, 182 21 Prague 8, Czechia
[3] National Research Tomsk Polytechnic University, Lenin Avenue, 30, Tomsk 634050, Russia

E-mail: milan.tichy@mff.cuni.cz

Received 11 September 2017, revised 20 November 2017
Accepted for publication 24 November 2017
Published 19 December 2017

**Abstract**

The floating harmonic probe is a relatively new plasma diagnostic method, which was proposed for applications at conditions when insulating films are deposited on the probe and, consequently, the classical Langmuir probe method fails. In the floating harmonic probe method a purely sinusoidal AC voltage is applied to the probe constructed in a standard manner via a capacitor. From the spectral components of the measured AC probe current waveforms, the electron temperature and the positive ion density can be obtained. In this contribution we present the comparison of the electron temperature and density acquired by the floating harmonic probe method with those obtained by the classical Langmuir probe. The experiments are performed in the flowing DC discharge in argon. In addition, the results from the floating harmonic probe method obtained during deposition of an insulating iron oxide thin film are shown. All the data is complemented by the qualitative discussion.

Keywords: plasma diagnostic, floating harmonic probe, Langmuir probe, hollow cathode, non-conducting film deposition

(Some figures may appear in colour only in the online journal)

## Introduction

The most widely used electric probes in low-temperature plasmas are the Langmuir probes (LPs). Many important plasma parameters can be extracted from the *I–V* characteristics of the single LP, such as the electron and ion density, electron temperature or the electron energy distribution function (EEDF). However, if used in conditions when badly conducting films are being deposited, this method in most cases fails as the resistance of the insulating film deposited on the probe's tip gets higher and the *I–V* characteristic renders distorted. In order to make possible the measurement of the basic plasma parameters, e.g. the electron density and the electron temperature, a range of probe methods that operate with an AC voltage have been developed to overcome this problem. One group of these methods is based on the high-frequency/microwave spectroscopy. In the case of the passive plasma resonance spectroscopy, the probe works as antenna that monitors existing oscillations of the plasma, and in the active plasma resonance spectroscopy the probe couples a suitable RF signal into the plasma and evaluates the corresponding frequency response [1, 2]. As a representative of the first group may serve e.g. the plasma oscillation probe [3], examples of the second group are the plasma impedance probe [4], the hairpin probe [5], the multipole resonance probe [6] and the curling probe [7]. All the mentioned probe methods determine the electron density and [6] also the electron temperature and the plasma collision frequency. An advantage of these methods is the possibility to monitor the plasma technological process (deposition, sterilization, etc.) continuously, without the need to measure and process the probe characteristic. A disadvantage of these methods is the need of microwave instrumentation (a vector network analyzer) and large size and comparatively complicated construction of all the probes

[4] Author to whom any correspondence should be addressed.


© 2017 IOP Publishing Ltd Printed in the UK

listed above. As a probe that utilizes an AC voltage at the RF frequency we mention the probe method for ion flux measurements [8]. This method is almost independent of the thickness of the non-conducting layer of the probe; however, for the method to work properly it is necessary to have a large flat probe (in [8] the diameter of the probe was 50 mm).

The idea to couple an AC signal into the DC probe bias was discovered a long time ago. An example of the application of this idea may serve the works [9, 10] where a second harmonic of a harmonic signal coupled into the probe circuit was used to measure the EEDF in a plasma of a striated discharge. The concept of the so-called floating harmonic probe (FHP), i.e. a method where only an AC signal is applied to the probe over a capacitor, was proposed already in [11] and was originally intended for direct-display of the electron temperature fluctuations in the edge plasma of tokamaks [12]. In [13] this technique has been extended to also evaluate the ion number density and it was proposed to be used in low-temperature processing plasmas, where the probe tip gets coated by an insulating layer. Up to now the FHP has been found useful e.g. during deposition of DLC thin films [14, 15] and the basic concept of FHP has been further utilized in double probe diagnostics [16], a method using sideband harmonics generated by dual-frequency input voltage [17, 18] or a method applicable to pulsed discharges with temporal resolution below 1 $\mu$s [19]. The case when the capacitive reactance of the deposited film is not negligible was treated in [20, 21].

## Principle of FHP operation

In the FHP method an AC voltage $V_0 \cos\omega t$ is applied to the probe, see figure 1. A capacitor is connected between the probe and the harmonic voltage source, so that no DC current can flow through the probe and the probe is floating at a certain potential $\bar{V}$ with respect to the plasma potential $\Phi_{\mathrm{pl}}$. The probe current is assumed to be a sum of the positive ion current and the electron current:

$$i = i^{+} - i^{-} \exp\left[\left(\bar{V} + V_0 \cos\omega t\right)/T_{\mathrm{e}}\right] \tag{1}$$

where $i^{-}$ is the electron current when the probe voltage equals to the plasma potential $\Phi_{\mathrm{pl}}$ and $e$ is the elementary charge. The ion current $i^{+}$ is supposed to be independent of the probe voltage and the EEDF is assumed to be Maxwellian with temperature $T_{\mathrm{e}}$. To make the equations simpler, we expressed in equation (1) as well as further in the text the electron temperature in volts. The periodic exponential term can be written [22] in terms of Bessel functions $I_k(z)$ of integer order $k$ as:

$$\mathrm{e}^{z\cos(\theta)} = I_0(z) + 2\sum_{k=1}^{\infty} I_k(z)\cos(k\theta).$$

Substituting the above expansion (with $\theta = \omega t$ and $z = V_0/T_{\mathrm{e}}$) into equation (1) the probe current reads [21]:

$$\begin{aligned} i =& i^{+} - i^{-}\exp\left(\bar{V}/T_{\mathrm{e}}\right) I_0\left(V_0/T_{\mathrm{e}}\right) \\ &- 2i^{-}\exp\left(\bar{V}/T_{\mathrm{e}}\right)\sum_{k=1}^{\infty} I_k\left(V_0/T_{\mathrm{e}}\right)\cos k\omega t. \end{aligned} \tag{2}$$

The AC component of the probe current is hence composed not only of the fundamental frequency $\omega$, but also currents at higher harmonic frequencies are generated due to the non-linear characteristics of the sheath. Note that by applying the AC voltage the probe no longer floats at its former floating potential $V_{\mathrm{f}}$. That is the effect known from the asymmetrically capacitively coupled RF discharges; on the driven electrode a DC self-bias is created with the magnitude:

$$\bar{V} = V_{\mathrm{f}} - T_{\mathrm{e}}\ln\left(I_0\left(\frac{V_0}{T_{\mathrm{e}}}\right)\right). \tag{3}$$

### *Determination of the electron temperature*

Since the probe is floating we can express the electron current in terms of the positive ion current and we obtain for the probe current the expression [12]:

$$\begin{aligned} i &= i^{+}\left\{\frac{2}{I_0\left(V_0/T_{\mathrm{e}}\right)}\sum_{k=1}^{\infty} I_k\left(V_0/T_{\mathrm{e}}\right)\cos\left(k\omega t\right)\right\} \\ &= \sum_{k=1}^{\infty} i_{k\omega}\cos\left(k\omega t\right); i_{k\omega} = 2i^{+}\frac{I_k\left(V_0/T_{\mathrm{e}}\right)}{I_0\left(V_0/T_{\mathrm{e}}\right)}. \end{aligned} \tag{4}$$

It follows that from the ratio of the amplitudes of the harmonic currents $i_{k\omega}$, the electron temperature $T_{\mathrm{e}}$ can be evaluated by numerical solution of the equation, see e.g. [12, 13, 20, 21]:

$$i_{n\omega}/i_{m\omega} = I_n\left(V_0/T_{\mathrm{e}}\right)/I_m\left(V_0/T_{\mathrm{e}}\right). \tag{5}$$

### *Determination of the positive ion density*

For the positive ion density evaluation a proper formula for the ion current $i^{+}$ must be employed. We have tested two collisionless theories: the radial Allen, Boyd and Reynolds theory (ABR) [23] and the Laframboise theory [24]. According to the ABR theory for cylindrical LP, the ion current at floating potential can be written as [25]:

$$i^{+} = \alpha e A_{\mathrm{p}} n_{\mathrm{i}}\sqrt{T_{\mathrm{e}}/M_{\mathrm{i}}} \tag{6}$$

where $A_{\mathrm{p}}$ is the probe area, $M_{\mathrm{i}}$ the ion mass, $n_{\mathrm{i}}$ the ion number density and $\alpha$ an effective Bohm coefficient. This coefficient depends on ion mass and the Debye number $D_\lambda$, the ratio of the probe radius to the Debye length $D_\lambda = r_{\mathrm{p}}/\lambda_{\mathrm{D}}$ and for argon ions can be computed by utilizing the analytical approximation from [25]. According to equation (4) the ion density $n_{\mathrm{i}}$ can be determined from the first harmonic current $i_{1\omega}$ by numerical solution of the expression:

$$n_i = \frac{i_{1\omega}}{2\alpha e A_{\mathrm{p}}\sqrt{T_{\mathrm{e}}/M_{\mathrm{i}}}}\frac{I_0\left(V_0/T_{\mathrm{e}}\right)}{I_1\left(V_0/T_{\mathrm{e}}\right)}. \tag{7}$$

In the case of the Laframboise theory the ion current $i^{+}$ was expressed by the analytical formula that can be found in [26] evaluated at the probe potential $\Phi_{\mathrm{pl}} - 5.2T_{\mathrm{e}}$. The ion density was determined in similar way from the first harmonic current using equation (4).

For the operation of the probe as described above, it is crucial that the capacitance of the sheath $C_{\mathrm{s}}$ can be neglected.

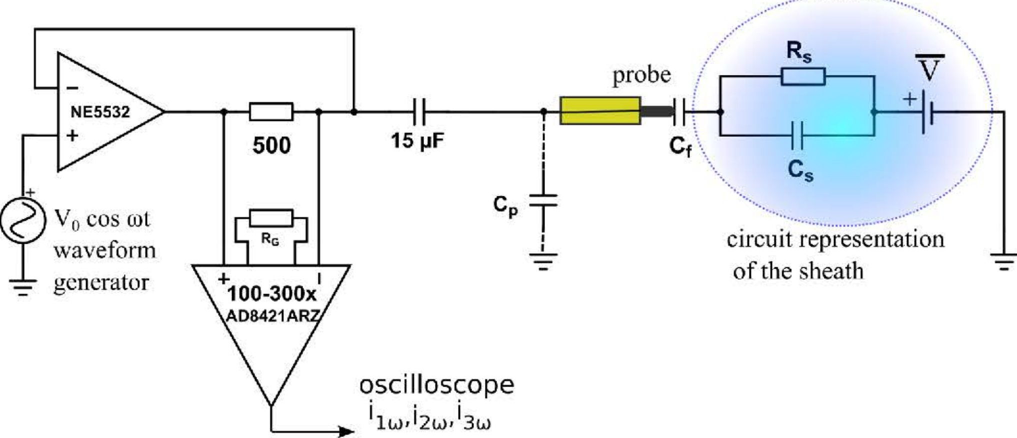


**Figure 1.** The scheme of the FHP measuring circuit including the linearized circuit representation of the sheath around the probe and the parasitic capacitance $C_p$.

This condition, however, limits the maximum operating frequency $\omega$ that can be used. Furthermore, the potential drop on the capacitance of the insulating film $C_f$ is in the above treatment also neglected, which limits the maximum thickness of the deposited insulating film. After introducing the real part of the impedance of the sheath $R_s$ as the first derivative of the probe $I$–$V$ characteristics at the potential $\bar{V}$ at which the FHP floats, $R_s^{-1} = \frac{dI}{dV}(\bar{V})$ [27], the range of operating frequencies of the FHP can be expressed by:

$$\omega C_f \gg 1/R_s \gg \omega C_s. \tag{8}$$

This is a vital condition that is indispensable to be fulfilled for the FHP to deliver reliable data. Failure to comply with this condition leads to faulty data as it will be shown later on in this work.

### Corrections on the capacitive reactance of the deposited film

When the above mentioned condition $\omega C_f \gg 1/R_s$ is not fulfilled, the input voltage is divided on the voltage divider consisting of the sheath impedance and the impedance of the film. Treating the film as a pure capacitor, the amplitude of the voltage across the sheath $V_S$ can be expressed as $V_S = V_0 \cos \varphi_1$, where $\varphi_1$ is the phase shift between the first harmonic current $i_{1\omega}$ and the input voltage $V_0$, see [20, 21]. The expressions for the ion density evaluation (4) and (7) using the first harmonic current $i_{1\omega}$ are then changed only by substituting $V_S$ for $V_0$, see [20, 21].

A different approach needs to be used, when evaluating the electron temperature, as the currents of higher harmonic frequencies are further diminished due to generation of voltage of higher harmonic frequencies on the impedance of the film and consequently on the sheath. In [20] it was proposed to utilize only the first harmonic currents $i_{1\omega,1}$ and $i_{1\omega,2}$ and corresponding phase shifts $\varphi_{1,1}$, $\varphi_{1,2}$ obtained from measurements with two different voltage amplitudes $V_{0,1}$ and $V_{0,2}$, respectively:

$$\frac{i_{1\omega,1}}{i_{1\omega,2}} = \frac{I_0(V_{0,2}\cos\varphi_{1,2}/T_e)\, I_1(V_{0,1}\cos\varphi_{1,1}/T_e)}{I_0(V_{0,1}\cos\varphi_{1,1}/T_e)\, I_1(V_{0,2}\cos\varphi_{1,2}/T_e)}. \tag{9}$$

In [21] a more detailed analysis of the circuit treating the deposited film as pure capacitance was made, from which it follows that the electron temperature can be obtained from the first $i_{1\omega}$ and second $i_{2\omega}$ harmonic currents and the respective phase shifts $\varphi_1$ and $\varphi_2$:

$$\frac{i_{1\omega}}{i_{2\omega}} = \frac{I_1(V_0\cos\varphi_1/T_e)}{I_2(V_0\cos\varphi_1/T_e)\,\cos(2\varphi_1-\varphi_2)}. \tag{10}$$

## Experimental arrangement

Measurements were carried out in the plasma plume of a DC discharge in a low-pressure (1–50 Pa) hollow cathode plasma jet sputtering system. In this system, argon gas flows through a tubular-shaped, water-cooled nozzle/hollow-cathode of length 29 mm and of inner diameter 5 mm made of pure Fe (99.99%). The nozzle is placed at the top of the cylindrical ultra-high vacuum chamber 30 cm in diameter and 30 cm in height, which is pumped by a combination of a mechanical and a turbo-molecular pump down to the ultimate pressure of $10^{-5}$ Pa. The hollow cathode is powered by a DC power supply Advanced Energy MDX 500 operating in a constant current mode. The outer surface of the nozzle is isolated from the discharge volume by a cylindrical shield made of a lava ceramic that prevents the burning of the discharge in any other part of the nozzle except the hollow cathode. The used plasma-jet deposition system is schematically drawn and described in more detail in [28]. For the deposition of iron oxide, the reactive gas $O_2$ was introduced to the reactor vessel by a lateral port to prevent the hollow-cathode from poisoning.

In order to make the experiment as general as possible, two different cylindrical probes made of tungsten wire: one 4 mm long and of diameter 50 $\mu$m (hereafter called the *thin* probe) and 3 mm long and 800 $\mu$m in diameter (hereafter called the *thick* probe) were used simultaneously and positioned near each other in the plasma plume at the system axis at the distance of 4 cm downstream from the nozzle exit perpendicular to the plasma flow. Both probes were used in the FHP regime as well as in the regime of a standard LP. In the latter regime of operation the $I$–$V$ characteristics

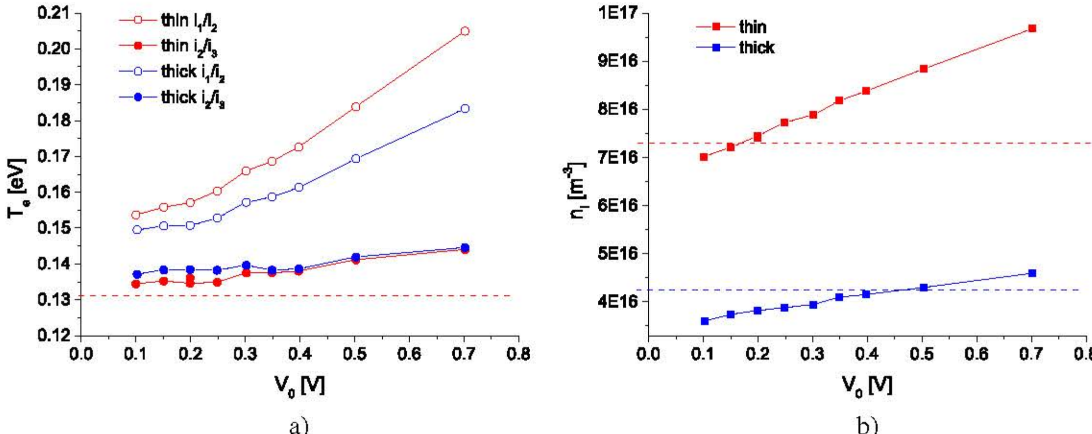


**Figure 2.** Dependence of the electron temperature (a) and ion density (b) according to the Laframboise theory obtained from FHP on the AC voltage amplitude $V_0$ for a fixed frequency of 20 kHz at conditions: $p = 7$ Pa, $Q_{Ar} = 120$ sccm, $I_v = 300$ mA. The dashed horizontal lines depict the results from $I$–$V$ characteristics.

were recorded using the Keysight B2901A Precision Source/Measure Unit.

The electric circuit employed for the FHP technique is depicted in figure 1. The probe current was sensed on a 500 $\Omega$ resistor and the current signal was amplified by a low noise, low bias current, high speed and high CMRR differential amplifier AD8421 by a factor of 100–300. The high CMRR allows the extraction of low level signals even in the presence of high frequency common-mode noise. As a signal recording and processing device, a digital oscilloscope Agilent DSO-X 2004A was used. The oscilloscope was operated in the acquisition mode that averaged over 64 waveforms. From the recorded waveforms, the amplitudes and phases of the harmonic currents were obtained using the discrete Fourier transform. The negative feedback line in the operational amplifier NE5532 was hooked up at the end of the sensing resistor as depicted in figure 1. This ensured that only the voltage of the fundamental frequency $\omega$ was applied on the probe tip and the amplitudes of higher frequencies generated on the sensing resistor were suppressed. To let the probe float and get it self-biased, a 15 $\mu$F capacitor was employed; with its capacitance sufficiently high to render the voltage drop on that negligible at all the used frequencies. Due to a parasitic capacitance of the probe shaft as well as of the measuring circuit itself to ground a parasitic current of the base frequency was observed even with the discharge off. This parasitic capacity was evaluated to $C_p \approx 30$ pF and the parasitic current was always subtracted from the obtained data.

## Results and discussion

The purpose of our experiment is to show the applicability of the FHP in the argon discharge and in the argon discharge containing admixture of oxygen when an insulating layer of iron oxide is deposited on the probe. In the former case the iron hollow cathode is also sputtered, however, the film deposited on the probe is conducting and does not affect substantially the probe dimensions. The plasma parameters that are obtained from the experimental data are the electron temperature $T_e$ and the positive ion density $n_i$. As a reference standard for comparison we use the data from the $I$–$V$ characteristics of both the probes. The comparison of the data from the FHP and from the processed $I$–$V$ characteristics was feasible only for the plasma of a discharge in pure argon.

In the following paragraphs we show the results of comparison of both the above mentioned plasma parameters dependent on the amplitude of the applied AC voltage, on its frequency and on the argon pressure. In addition, plasma parameters were measured with approximately 3% admixture of oxygen in argon dependent on time for about 3/4 h in 3 min intervals with only FHP. In this experiment, they serve as the reference for the plasma parameters measured by the FHP before the $O_2$ flow was started and after the $O_2$ flow was stopped. It is necessary to stress that by changing the amplitude or the frequency of the applied voltage we do not influence the plasma; the data on the $T_e$ and $n_i$ determined from the FHP are given to show how accurate the FHP stands in comparison with a standard LP.

### *Dependence of the $T_e$ and $n_i$ measured by FHP on the applied voltage amplitude*

The measurements were made at first in an argon discharge, i.e. without oxygen (no insulating layer was deposited); to discover the FHP behaviour and to compare the plasma parameters obtained from the FHP data with those from the LP. The dependence of the electron temperature $T_e$ on the AC voltage amplitude $V_0$ at a fixed frequency of 20 kHz, discharge current 300 mA and argon pressure 7 Pa can be seen in figure 2(a). The electron temperature was evaluated according to the equation (5) using both the ratio of the first to the second harmonic current component $i_{1\omega}/i_{2\omega}$, as well as the ratio of the second to the third harmonic current component $i_{2\omega}/i_{3\omega}$. It can be seen that the value of the electron temperature obtained from $i_{2\omega}/i_{3\omega}$ is slightly lower and is in rather good agreement with the value of the electron temperature obtained from the $I$–$V$ characteristics, which is depicted as the horizontal dashed line. It can be clearly seen that the dependence on $V_0$ is much more pronounced in case of the electron temperature obtained from $i_{1\omega}/i_{2\omega}$. This can be

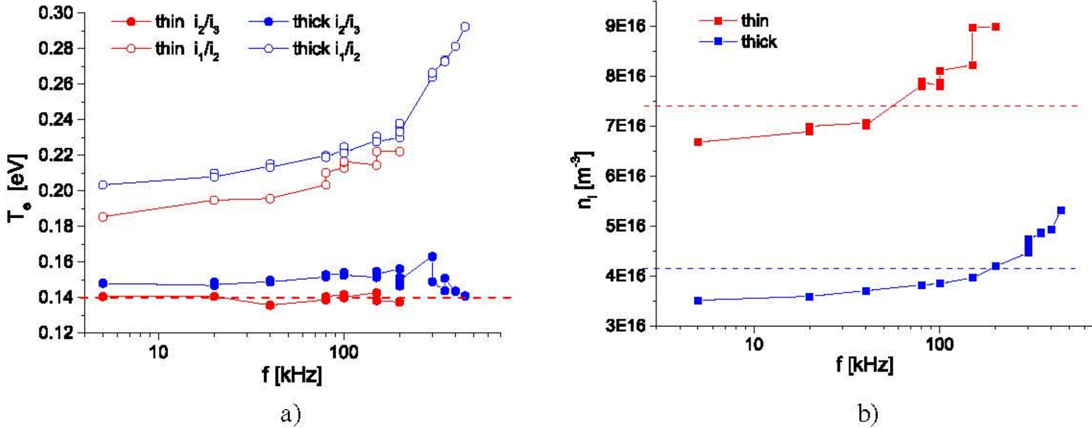


**Figure 3.** Dependence of the electron temperature (a) and ion density (b) according to the Laframboise theory obtained from FHP on the frequency for a fixed AC voltage amplitude $V_0 = 0.25$ V at conditions: $p = 5$ Pa, $Q_{\mathrm{Ar}} = 100$ sccm, $I_{\mathrm{v}} = 300$ mA. The dashed horizontal lines depict the results from $I$–$V$ characteristics.

explained by the fact, that the ion current is not independent on the probe voltage and therefore some AC ion current is generated, which contributes to the measured current, predominantly to the first harmonic current component $i_{1\omega}$ [29]. Somewhat surprisingly, there is not much difference between the thick and the thin probe in the slope of the trends. The slightly rising trend of the electron temperature obtained from $i_{2\omega}/i_{3\omega}$ might be also caused by the self-biasing effect. As the AC voltage $V_0$ increases, the FHP floating potential $\bar{V}$ gets more negative because of the self-bias and due to the possible non-Maxwellian tail of the EEDF in an argon discharge at low pressure (see e.g. [30]), the obtained electron temperature can be overestimated.

The ion density according to the Laframboise theory obtained from FHP dependent on the AC voltage $V_0$ is shown in figure 2(b). For the calculation, the electron temperature obtained from $i_{2\omega}/i_{3\omega}$ was used. The dashed lines depict the ion density obtained from the respective $I$–$V$ characteristics according to the Laframboise theory (with the working point chosen at $\Phi_{\mathrm{pl}} - 20T_{\mathrm{e}}$). The comparatively large difference between the ion densities determined in the same plasma at rather low pressure by the probes with a different diameter is probably caused by the flowing medium. At the rather high throughput 120 sccm and the low pressure 7 Pa the plasma flow velocity becomes comparable to the thermal velocity [31]. That reduces the ion collection efficiency at the downstream side of the thick probe—shadow effect—hence reducing the effective collection area of the thick probe. Moreover, similar effect can cause the possible anisotropy of the EEDF [32]. Consequently, without a proper correction to that effect, the apparent ion density comes out smaller both in the case of the ion density evaluation from the FHP as well as from the $I$–$V$ characteristic. As the ion density is determined from the first harmonic current, the obtained rising trend of the ion density with increasing $V_0$ is likely caused by the AC ion current and the self-biasing effect. For low AC voltage amplitudes $V_0$, lower than approximately $2T_{\mathrm{e}}$, the data from the FHP can be assessed to be in reasonably good agreement (20% error) with the results from $I$–$V$ characteristics.

### *Dependence of the $T_{\mathrm{e}}$ and $n_i$ measured by FHP on the applied voltage frequency*

The dependence of the electron temperature and the ion density determination on the frequency of the applied AC voltage was also investigated; the results can be seen in Figures 3(a) and (b). The difference between the ion densities of the thick and thin probe may be again attributed to the shadowing effect. The increase of the obtained values with frequency can account for the increase of the first harmonic current due to the sheath capacitance, since the right part of the inequality (8) at higher frequencies may not hold anymore.

It can be seen in figure 3(a) that the dependence of $T_{\mathrm{e}}$ on the frequency is much more pronounced in the case of the electron temperature obtained from the ratio $i_{1\omega}/i_{2\omega}$. The results displayed in figure 3(a) also indicate that the electron temperature $T_{\mathrm{e}}$ obtained from the ratio $i_{2\omega}/i_{3\omega}$ corresponds reasonably well to the $T_{\mathrm{e}}$ value obtained from the standard LP characteristic (the data from the thin and the thick probe correspond to each other; indicated by red line) and that it does not seem to be too influenced by the sheath capacitance in the studied frequency range.

### *Dependence of the $T_{\mathrm{e}}$ and $n_i$ measured by FHP on the argon pressure*

Figures 4 and 5 show the comparison of the data on $T_{\mathrm{e}}$ and $n_{\mathrm{i}}$ obtained from the FHP with the LP method in a wider range of conditions, as the argon pressure in the chamber was changed. The electron temperature from FHP using the ratio $i_{2\omega}/i_{3\omega}$ depicted in figure 4(a) is in a very good agreement with the electron temperature of the body of the EEDF, obtained from $I$–$V$ characteristics using the Druyvesteyn formula [33], except for pressures less than about 2 Pa, where the EEDF has been found bi-Maxwellian. At these low pressures the obtained electron temperature is in accordance with the temperature obtained from the linear approximation of the tail of the EEDF; see figure 4(b). The fact that the FHP is, at certain experimental conditions,

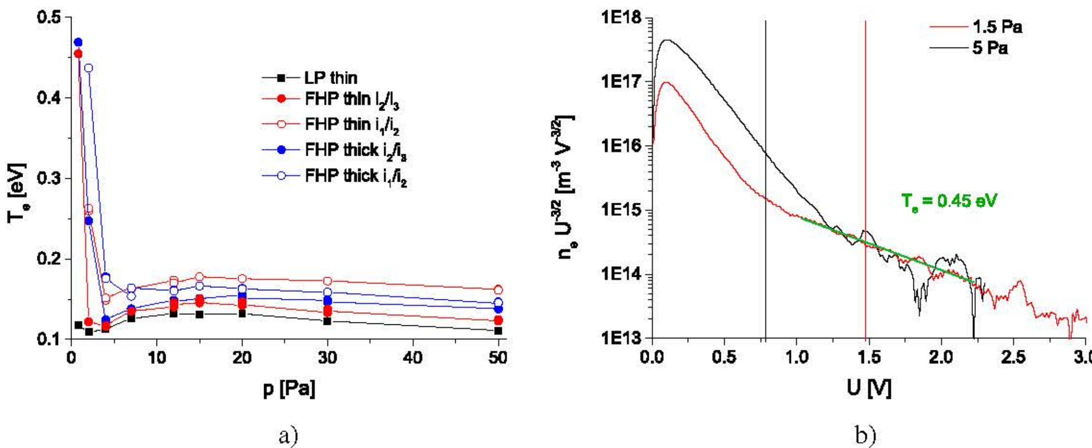


**Figure 4.** Pressure dependence of the electron temperature. (a) A frequency of 20 kHz and AC voltage amplitude of 0.25 V was used. Conditions: $Q_{\mathrm{Ar}} = 120$ sccm, $I_{\mathrm{v}} = 300$ mA. (b) The measured EEDF at two different pressures 1.5 and 5 Pa. The vertical bars show the floating potential of the probes around which the AC voltage was applied at the two indicated pressures.

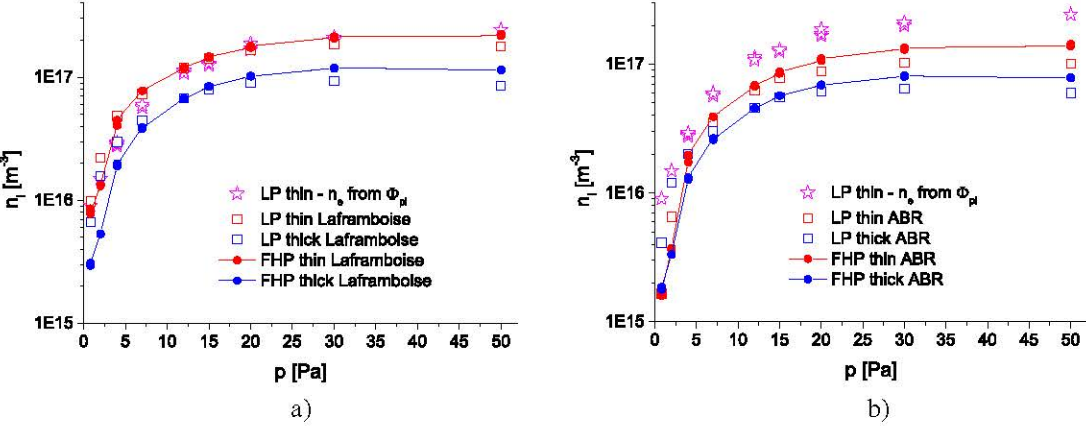


**Figure 5.** Pressure dependence of the ion density determined using the theory of Laframboise (a) and the Allen, Boyd and Reynolds theory (b) using both the FHP and the LP ($I$–$V$ characteristics) method. The stars depict the electron density determined by the thin LP. A frequency of 20 kHz and AC voltage amplitude of 0.25 V was used. Conditions: $Q_{\mathrm{Ar}} = 120$ sccm, $I_{\mathrm{v}} = 300$ mA.

theoretically capable of measuring the temperature of the linear approximation of the tail of the EEDF at the electron energy corresponding to the floating potential, it can be readily seen that the electron current in (1) is expressed using the temperature of the linear approximation of the tail of the EEDF.

As far as the estimation of the ion density $n_{\mathrm{i}}$ is concerned, one has to be aware of the effect of the collision of ions with neutral particles in the probe sheath. Since we were interested in a gross comparison between the FHP and the LP data, we plotted in figure 5 the ion density data obtained without taking collisions into account. Ion density obtained from the two ion current theories are shown as follows: in figure 5(a) the Laframboise theory [24] and in figure 5(b) the ABR theory [23]. For comparison, the $n_e$ data estimated from the electron probe current at plasma potential are plotted in figures 5(a) and (b). The difference in $n_{\mathrm{e}}$ between the thick and thin probe was maximally 20%, hence only one plot of $n_{\mathrm{e}}$ is shown. The plasma potential was determined as the abscissa of the zero-crossing of the second derivative of the $I$–$V$ characteristics with respect to the probe voltage and also agreed very well between the thin and the thick probe.

It can be seen that the ion density obtained using the FHP method agrees well with the data from the respective $I$–$V$ characteristics (LP) for both the thick and thin probe regardless of which ion current theory was used. However, at lower pressures when the EEDF is not Maxwellian, and probably also anisotropic [32], the density from FHP is underestimated up to a factor of two. The ion density determined using the Laframboise theory fits well with the electron density data in the case of the thin probe, however, the ion density is underestimated in the case of the thick probe at low pressures due to the shadowing effect [31, 32] and at higher pressures due to the ion collisions in the sheath. For instance at 20 Pa the ratio of the sheath thickness calculated according to [34] and the ion mean free path is about 0.7 for the thick probe whereas it is only 0.35 for the thin probe. The ion density obtained using the ABR theory is underestimated compared to the electron density in the whole pressure range. This has been reported also by other authors, see e.g. [35].

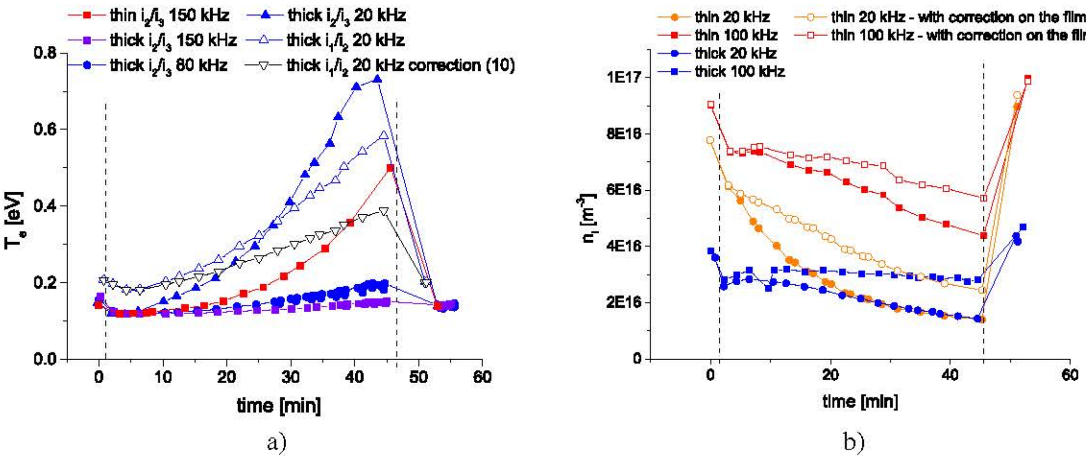


**Figure 6.** The electron temperature (a) and ion density (according to Laframboise) (b) obtained from FHP. During the time interval delimited by the vertical lines, oxygen was being fed with the flow of 3 sccm and an iron oxide thin film was being deposited. A fixed AC voltage amplitude of 0.25 V was used with various frequencies. Conditions: $p = 5$ Pa, $Q_{\mathrm{Ar}} = 100$ sccm, $I_{\mathrm{v}} = 300$ mA.

*Measurements by FHP at the presence of an insulating layer on the probe*

The results of measurements with FHP with the oxygen gas introduced into the discharge chamber and an insulating layer deposited on the probes are shown in figure 6. After about 45 min of deposition of the iron oxide on the probes, the oxygen flow was turned off and the probes were cleaned by ion bombardment in a pure argon discharge for about 5 min when biased at $-100$ V with respect to ground. A rather good agreement of the electron and the ion density obtained after probe cleaning with the values obtained before deposition—less than about 20%—indicate a satisfactory reproducibility of our measurement.

The *I–V* characteristics were also recorded during deposition; however, after less than 3 min the characteristics were distorted and after 10 min the ion current dropped by almost one order of magnitude. The results in figure 6 clearly show that for longer deposition times (thicker layer) a higher frequency must be utilized to satisfy the left part of the condition (8) and to obtain unperturbed data. It should be noted that for the evaluation of the ion density, the unperturbed electron temperature value was used. Looking at the electron temperature obtained, it can be seen that at these particular conditions using the thick probe at the frequencies of about 100 kHz and higher, the data can be said to be reliable even after 45 min of deposition. On the other hand the electron temperature obtained by means of the thin probe is almost five times higher than the temperature from the thick probe at the same frequency of 150 kHz. This may be explained by comparing the quantity $R_{\mathrm{S}}A_{\mathrm{p}}$—the sheath impedance multiplied by the respective probe area, which does not depend on the probe area. This quantity is not equal for the thin and thick probe, yet the one of the thick probe is larger. The reason is that the ion current normalized to the respective probe area is higher for the thin probe and the floating potential of the thin probe is therefore more positive. From the derivative of the *I–V* characteristics before deposition, the product of the sheath resistance and the probe area $R_{\mathrm{S}}A_{\mathrm{p}}$ at floating potential was evaluated to 0.2 kΩ cm$^2$ for the thin probe and 1.2 kΩ cm$^2$ for the thick probe, respectively.

**Table 1.** Rough estimation of characteristic parameters $C_{\mathrm{f}}$ and $Z_{\mathrm{f}}$ of the 1.1 $\mu$m thick $Fe_2O_3$ film on the thin and the thick probe @150 kHz and of the impedance $R_{\mathrm{s}}$ of the sheath around the probes.

| Probe | Thin | Thick |
|---|---|---|
| Film capacitance $C_{\mathrm{f}}$ | 7 pF | 66 pF |
| Film capacitive reactance $Z_{\mathrm{f}}$ @150 kHz | 160 kΩ | 16 kΩ |
| Sheath impedance $R_{\mathrm{s}}$ | 42 kΩ | 23 kΩ |

Having in mind the self-biasing effect, these results are in consent with the sheath resistance obtained directly at the mean FHP potential as $V_0/i_{1\omega}$. After the oxygen was introduced, the ion density decreased and the value $R_{\mathrm{s}}A_{\mathrm{p}}$ changed to 0.3 kΩ cm$^2$ for the thin probe and 1.5 kΩ cm$^2$ for the thick probe. The final thickness of the layer after deposition was roughly 1.1 $\mu$m. When treating the film on the probe as a planar capacitor, the capacitive reactance multiplied by the probe area at 150 kHz is roughly 1 kΩ cm$^2$ using the value of the relative permittivity of iron oxide of 1.3 from [36]. Table 1 shows these quantities calculated over the total area of the thin and the thick probe, respectively. Taking into account the requirement (8) rewritten in terms of impedances $Z_{\mathrm{f}} \ll R_{\mathrm{s}} \ll Z_{\mathrm{s}}$ we see that this condition is much better fulfilled for the thick probe than for the thin probe.

We have also evaluated the data taking into account the reactive capacitance of the film according to the model presented in [21], which are presented in figure 6. It can be clearly seen that in our experiment after employing the corrections the results are less perturbed, however, the corrections are not sufficient. Similar results were obtained also using a lower amplitude of the applied AC voltage of 0.15 V.

## Conclusion

We have utilized the FHP method using two cylindrical probes with different diameters in a plasma flow generated by a DC discharge in argon. We have compared the electron temperature and the electron density estimated from the FHP data with that when the probes were applied as conventional LPs. It was shown that the method for the electron temperature evaluation

from the FHP using the ratio of the second to the third harmonic current components gives a better agreement with the LP data compared to the $T_e$ values calculated from the ratios of the first to the second harmonic current component. That applies in the wide range of the amplitudes of the applied AC voltage, the operating frequency and the pressure. Furthermore it follows from our study that this method for the electron temperature evaluation from FHP seems to be almost unaffected by the sheath capacitance within the studied frequency range. The positive ion density data evaluated from the FHP and from the respective *I–V* characteristics using the Laframboise and the ABR theory were in fair agreement. From the results during deposition of iron oxide thin film, it followed that the thicker probe made possible the measurements with thicker deposited layers, i.e. when the data from the thin probe were already perturbed by the impedance of the insulating film and when the conventional LP method was unusable. We plan to apply the FHP method also during deposition of other non-conducting materials, e.g. $TiO_2$.

## Acknowledgments

This work was partially financially supported by the Czech Science Foundation by the project 15-00863S. Financial support by Charles University Grant Agency, grant no. 268115 is gratefully acknowledged.

## ORCID iDs

M Zanáška https://orcid.org/0000-0002-6855-9930
Z Hubička https://orcid.org/0000-0002-4051-057X
M Čada https://orcid.org/0000-0001-6826-983X
P Kudrna https://orcid.org/0000-0001-5948-4765
M Tichý https://orcid.org/0000-0003-4024-4838

## References

[1] Braithwaite N S J and Franklin R N 2009 *Plasma Sources Sci. Technol.* **18** 014008
[2] Lapke M *et al* 2011 *Plasma Sources Sci. Technol.* **20** 042001
[3] Schwabedissen A, Soll C, Brockhaus A and Engemann J 1999 *Plasma Sources Sci. Technol.* **8** 440–7
[4] Blackwell D D, Walker D N and Amatucci W E 2005 *Rev. Sci. Instrum.* **76** 023503
[5] Piejak R B, Godyak V A, Garner R and Alexandrovich B M 2004 *J. Appl. Phys.* **95** 3785
[6] Schulz C, Styrnoll T, Awakowicz P and Rolfes I 2015 *IEEE Trans. Instrum. Meas.* **64** 857
[7] Pandey A, Sakakibara W, Matsuoka H, Nakamura K and Sugai H 2014 *Appl. Phys. Lett.* **104** 024111
[8] Braithwaite N St J, Booth J P and Cunge G 1996 *Plasma Sources Sci. Technol.* **5** 677
[9] Boyd R L F and Twiddy N D 1959 *Proc. R. Soc.* A **250** 53
[10] Rayment S W and Twiddy N D 1969 *J. Phys. D: Appl. Phys.* **2** 1747
[11] Van Nieuwenhove R and Van Oost G 1988 *Rev. Sci. Instrum.* **59** 1053
[12] Boedo J A, Gray D, Conn R W and Luong P, Schaffer M, Ivanov R S, Chernilevsky A V, Van Oost G 1990 *Rev. Sci. Instrum.* **70** 2997
[13] Lee M-H, Jang S-H and Chung C-W 2007 *J. Appl. Phys.* **101** 033305
[14] Pang J and Lu W, Xin Y, Wang H, He J and Xu J 2012 *Plasma Sci. Technol.* **14** 172
[15] Bai Y, Li J, Xu J, Lu W, Wang Y and Ding W 2016 *Plasma Sci. Technol.* **18** 58
[16] Oh S-J and Choi I-J, Kim J-Y and Chung C-W 2012 *Meas. Sci. Technol.* **23** 085001
[17] Jang S, Kim G and Chung C 2011 *Thin Solid Films* **519** 7042
[18] Kim D, Lee H, Kim Y and Chung C 2013 *Appl. Phys. Lett.* **103** 084103
[19] Kim Y-S and Kim D-H, Lee H-C and Chung C-W 2015 *J. Appl. Phys.* **117** 243302
[20] Bang J-Y, Yoo K, Kim D-H and Chung C-W 2011 *Plasma Sources Sci. Technol.* **20** 065005
[21] Kim K-H, Kim D-H and Chung C-W 2017 *Plasma Sources Sci. Technol.* **26** 025001
[22] Abramowitz M and Stegan I A 1972 *Handbook of Mathematical Functions* (New York: Dover) p 376
[23] Allen J E, Boyd R L F and Reynolds P 1957 *Proc. Phys. Soc.* B **70** 297
[24] Laframboise G 1966 Theory of spherical and cylindrical Langmuir probes in a collisionless, Maxwellian plasma at rest *UTIAS Report* No. 100 University of Toronto, Institute of Aerospace Studies
[25] Chen F F and Arnush D 2001 *Phys. Plasmas* **8** 5051
[26] Chudacek O, Kudrna P, Glosík J, Šícha M and Tichý M 1995 *Contrib. Plasma Phys.* **35** 503
[27] Hershkowitz N 1989 How Langmuir probes work *Plasma Diagnostics* vol 1 eds O Auciello and D L Flamm (New York: Academic)
[28] Perekrestov R, Kudrna P and Tichý M 2015 *Plasma Sources Sci. Technol.* **24** 035025
[29] Lee J, Kim K-H and Chung C-W 2015 *Phys. Plasmas* **22** 123503
[30] Godyak V A, Piejak R B and Alexandrovich B M 1992 *Plasma Sources Sci. Technol.* **1** 36
[31] Kluson J, Kudrna P and Tichy M 2013 *Plasma Sources Sci. Technol.* **22** 015020
[32] Klagge S and Lunk A 1991 *J. Appl. Phys.* **70** 99
[33] Druyvesteyn M J 1930 *Z. Phys.* **64** 781
[34] Basu J and Sen C 1973 *Japan. J. Appl. Phys.* **12** 1081
[35] Chen F F, Evans J D and Zawalski W 2012 *Plasma Sources Sci. Technol.* **21** 055002
[36] Shinde S S *et al* 2011 *J. Semiconduct.* **32** 013001